

## Original Research Article

# Exploring the action of new FimH inhibitors against CTX-15 enzyme by enzoinformatics approach: A plausible arsenal against drug-resistant uropathogenic bacterial strains

Amir Saeed<sup>1,2\*</sup>, Khalid Alshaghдали<sup>1,3</sup>, Mohd Saeed<sup>3</sup>, Mousa Alreshidi<sup>3,4</sup>

<sup>1</sup>Department of Clinical Laboratory Sciences, College of Applied Medical Sciences, University of Hail, Hail, Saudi Arabia,

<sup>2</sup>Department of Medical Microbiology Faculty of Medical Laboratory Sciences, University of Medical Sciences & Technology, Khartoum, Sudan, <sup>3</sup>Molecular Diagnostic and Personalized Therapeutic Unit, University of Hail, Hail, Saudi Arabia, <sup>4</sup>Department of Biology, College of Sciences, University of Hail, Hail, Saudi Arabia

\*For correspondence: **Email:** [am.saeed@uoh.edu.sa](mailto:am.saeed@uoh.edu.sa); [mo.saeed@uoh.edu.sa](mailto:mo.saeed@uoh.edu.sa); **Tel:** +966-543099741

Sent for review: 24 September 2020

Revised accepted: 6 October 2021

### Abstract

**Purpose:** To explore the potency of FimH inhibitors against CTX-M  $\beta$ -lactamase enzyme type 15, in view of the increasing prevalence of CTX-M 15 in uropathogenic strains which has reduced the treatment options to minimal.

**Method:** FimH inhibitors were targeted against CTXM-15 by a molecular docking approach. Thereafter, the best ligand-target confirmation was selected and analyzed using LIGPLOT+ Version v.2.1. The hydrophobic and hydrogen bonding among the catalytic site amino acids of CTXM-15 and the FimH inhibitors were analyzed and 3-D structures were converted into 2-D images by LIGPLOT algorithm.

**Results:** Out of all the FimH inhibitors tested, 3'-chloro-4'- ( $\alpha$ -D-mannopyranosyloxy) biphenyl-4-carbonitrile, para-biphenyl-2-methyl-3'-methylamidemannoside, para-biphenyl-2-methyl-3',5'-dimethylamide- $\alpha$ -D-mannoside, and thiazolylamino mannoside exhibited better interaction with the CTX-M 15 active site than the positive control avibactam. Moreover, in CTX-M 15, the amino acid residues, Ser70, Tyr105, Ser130, Asn132, Thr216, Thr235, Gly236, and Ser237 were commonly interacting with these FimH inhibitors as well as avibactam.

**Conclusion:** The predicted findings suggest that these FimH inhibitors could be explored as potential CTX-M 15 inhibitors to cope-up with resistance issues of uropathogenic bacteria in the form of an alternate strategy.

**Keywords:** Antibiotic resistance, CTX-M 15 enzyme, Extended-spectrum  $\beta$ -lactamases, FimH, Urinary tract infections, Uropathogenic bacteria

This is an Open Access article that uses a funding model which does not charge readers or their institutions for access and distributed under the terms of the Creative Commons Attribution License (<http://creativecommons.org/licenses/by/4.0>) and the Budapest Open Access Initiative (<http://www.budapestopenaccessinitiative.org/read>), which permit unrestricted use, distribution, and reproduction in any medium, provided the original work is properly credited.

Tropical Journal of Pharmaceutical Research is indexed by Science Citation Index (SciSearch), Scopus, International Pharmaceutical Abstract, Chemical Abstracts, Embase, Index Copernicus, EBSCO, African Index Medicus, JournalSeek, Journal Citation Reports/Science Edition, Directory of Open Access Journals (DOAJ), African Journal Online, Bioline International, Open-J-Gate and Pharmacy Abstracts

## INTRODUCTION

Globally, around 150 million individuals suffer from urinary tract infections (UTI) each year, and its occurrence is neither gender-specific nor age-

dependent [1,2]. The causal bacteria in most UTI cases belong to the *Enterobacteriaceae* family [3], and the prevalence of extended-spectrum  $\beta$  lactamases (ESBLs) in this family has hindered the treatment options [4-6]. ESBLs of the

(Cefotaximase-Munich) CTX-M type, particularly CTX-M 15 enzyme, has become more common in clinical samples [5,7]. Thus, CTX-M 15 enzyme was selected as a target for performing the docking analysis in the present study.

On the other hand, in any infection process, adherence of bacteria to the mucosal surface of the host is usually the first crucial step, and this statement holds true in the case of UTI caused by *Enterobacteriaceae* species [8]. The uropathogenic strains of the *Enterobacteriaceae* family have type-1 fimbriae as an adhesive organelle. The FimH protein Hung is present at the end of type-1 fimbriae that is utilized by the bacteria for host cell attachment [9,10]. Various studies have suggested that type-1 fimbriae or FimH play a crucial role in the UTI caused by *Escherichia coli* and *Klebsiella pneumoniae* [11-14]. Thus, the advantages of using FimH inhibitors over the currently used antibiotics are their specificity for some bacterial species' particular adherence process, no effect on host microflora, and, most importantly, no resistance issues as it interferes with a bacterial attachment without bactericidal action [9]. The majority of FimH inhibitors structures were formulated using x-ray crystallographic findings such as 8-(methoxycarbonyl)octyl- $\alpha$ -D-mannoside, heptyl  $\alpha$ -D-mannopyranoside, para-biphenyl-2-methyl-3',5'-di-methylamide- $\alpha$ -D-mannoside, para-biphenyl-2-methyl-3'-methylamide mannoside, 3'-chloro-4'-( $\alpha$ -D-mannopyranosyloxy)biphenyl-4-carbonitrile, and thiazolylamino mannoside [9, 15-17]. In the present study, all these FimH inhibitors were selected to target the CTX-M 15-type ESBLs by applying the enzoinformatics approach. The findings suggested that FimH inhibitors might also be used against uropathogenic CTX-M 15 (ESBLs)-producing resistant bacteria.

They serve two purposes: (1) Hinder the attachment of uropathogenic strains, and (2) Avoid resistance due to CTX-M 15. However, wet-lab experimental analysis is needed to establish the findings of the present study. Nonetheless, these FimH inhibitors could be explored further to transform the status of the antibiotic therapy regimen for UTI treatment.

## METHODS

### FimH inhibitors, avibactam and target protein structure retrieval

FimH inhibitors three-dimensional structure were obtained from the 'FimH-inhibitors' complex present in protein data bank. The FimH inhibitors used for the study were 8-

(Methoxycarbonyl)octyl- $\alpha$ -D-mannoside [PDB ID: 4AVI], Heptyl  $\alpha$ -D-mannopyranoside [PDB ID: 4BUQ], 3'-Chloro-4'-( $\alpha$ -D-mannopyranosyloxy) biphenyl-4-carbonitrile [PDB ID: 4CST], para-Biphenyl-2-methyl-3'-methylamidemannoside [PDB ID: 5F3F], para-Biphenyl-2-methyl-3',5'-di-methylamide- $\alpha$ -D-mannoside [PDB ID: 5F2F], and Thiazolylaminomannoside [PDB ID: 5MTS]. Target protein structure of 'Cefotaximase-Munich 15 (CTX-M 15)' [PDB ID: 4S2I] was also obtained from a Protein Data Bank. However, positive control avibactam [CID: 9835049] 3D structure was retrieved from PubChem database.

### Physicochemical properties and toxicity potential prediction

The physicochemical properties and toxicity potential of FimH inhibitors and positive control were estimated by using the Osiris Datawarrior property explorer tool.

Initially, different physicochemical parameters such as no. of hydrogen bond acceptors and donors, cLogP value, molecular weight, topological polar surface area, number of rotatable bonds, and the Lipinski's rule violation [18] were calculated. Thereafter, absorption was estimated as in Eq 1 [19].

$$\text{Absorption \%} = 109 - (0.345 \times \text{TPSA}) \dots \dots \dots (1)$$

Prediction of toxicity was also evaluated by the orisis datawarrior tool, in which predictions are based on comparative analysis of our tested compounds with the pre-estimated set of known structural molecules. Mutagenicity, tumorigenicity, reproductive effects and irritability features of our tested compounds were predicted for toxicity assessment.

### Molecular docking

'FimH inhibitors and avibactam' were considered as ligands and docked to target protein 'CTX-M 15' by following Rizvi *et al* protocol [20]. Each ligand energy was minimized by applying the MMFF94 force field, followed by gasteiger charges addition. Rotatable bonds were specified after adding non-polar hydrogen atoms. Kollman united atom type charges, solvation parameters, and hydrogen atoms were added using AutoDock 4.2. Autogrid was used to keep 60 x 60 x 60 Å as a grid dimension, with points separated by 0.375 Å. For explicitly targeting the 'CTX-M 15 catalytic site', the values of x, y, and z coordinates were kept as 6.930, 14.060, 9.920. Electrostatic and Van der Waals parameters

were estimated by applying dielectric functions and default parameters of AutoDock 4.2. 'Lamarckian and Solis and Wets local' algorithm was used to perform molecular docking experiments. One hundred different runs were applied for each docking experiment that was further set to end after 2,500,000 energy evaluations, and population size was kept as 150. At the end, final AutoDock 4.2 figures were studied using Discovery Studio 2.5 (Accelrys).

### LIGPLOT+ analysis of docked results

After performing the docking, the best ligand-target confirmation was selected and analyzed using LIGPLOT+ Version v.2.1. The hydrophobic and hydrogen bonding among the catalytic site amino acids of CTXM-15 and the FimH inhibitors were analyzed and 3-D structures were converted into 2-D images by LIGPLOT algorithm.

## RESULTS

In the present study, six FimH inhibitors, namely 8-(methoxycarbonyl)octyl- $\alpha$ -D-mannoside; heptyl  $\alpha$ -D-mannopyranoside; para-biphenyl-2-methyl-3',5'-di-methyl amide- $\alpha$ -D-mannoside; 3'-chloro-4'-( $\alpha$ -D-mannopyranosyloxy)biphenyl-4-carbonitrile; para-biphenyl-2-methyl-3'-methyl amide mannoside and thiazolylamino mannoside were chosen to target CTX-M 15 using molecular docking approach. Prior to molecular interaction study, the physicochemical properties and toxicity potential of these inhibitors were evaluated (Table 1 and Table 2). In the physicochemical property assessment, 8-(methoxycarbonyl)octyl- $\alpha$ -D-mannoside; thiazolylamino mannoside and para-biphenyl-2-methyl-3',5'-di-methylamide- $\alpha$ -D-mannoside did not adhere to one of the "Lipinski's rule of five" in terms of the number of rotatable bonds, hydrogen bond acceptors and donors, respectively (Table 1). On the other hand, out of all the FimH inhibitors tested, only 3'-chloro-4'-( $\alpha$ -D-mannopyranosyloxy)biphenyl-4-carbonitrile exhibited high toxicity with mutagenic, tumorigenic, reproductive, and irritant effects (Table 2), whereas the positive control avibactam exhibited mutagenic and irritant effects.

Molecular docking study revealed Gibbs free energy change ( $\Delta G$ ) and inhibition constant ( $K_i$ ) of 'FimH inhibitors' interaction with 'CTX-M 15 enzyme' (Table 3). The  $\Delta G$  and  $K_i$  values for the interaction between 3'-chloro-4'-( $\alpha$ -D-mannopyranosyloxy) biphenyl-4-carbonitrile and CTX-M 15 were -7.46 kcal/mol and 3.38 mM, respectively (Table 3). Amino acid residues of CTX-M 15 interacted with 3'-chloro-4'-( $\alpha$ -D-

mannopyranosyloxy)biphenyl-4-carbonitrile were Ser70, Asn104, Tyr105, Tyr129, Ser130, Asn132, Pro167, Asn170, Thr171, Thr216, Lys234, Thr235, Gly236, Ser237, Gly238, and Gly240. LIGPLOT showed that Ser130, Lys234, and Thr235 amino acids of CTX-M 15 were involved in hydrogen bonding, whereas Ser70, Asn104, Tyr105, Tyr129, Asn132, Pro167, Asn170, Thr171, Thr216, Gly236, Ser237, Gly238, and Gly240 were involved in hydrophobic interactions (Figure 1). Furthermore, the total intermolecular energy for the interaction was -8.66 kcal/mol, while, 'Van der Waals + Hydrogen bond + Desolvation energy' were -8.52 kcal/mol with electrostatic energy of -0.14 kcal/mol.

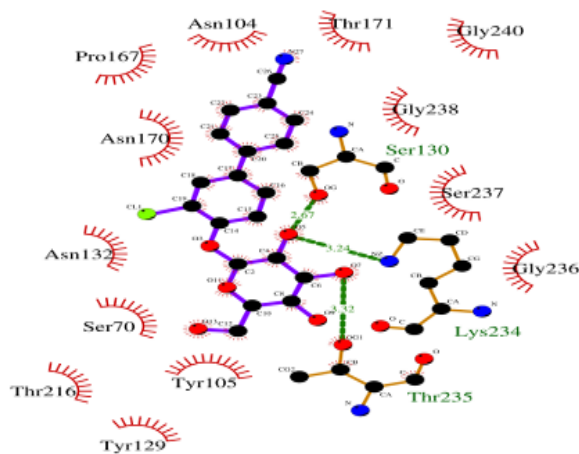


**Figure 1:** Ligplot analysis of '3'-chloro-4'-( $\alpha$ -D-mannopyranosyloxy) biphenyl-4-carbonitrile' - 'CTX-M 15' interaction. Red arcs represents the amino acid involved in hydrophobic interactions, whereas, green dashed lines represents the hydrogen bonds along with bond lengths

CTX-M 15 interaction results with para-biphenyl-2-methyl-3',5'-di-methylamide- $\alpha$ -D-mannoside showed  $K_i$  and  $\Delta G$  values of 2.54 mM and -7.63 kcal/mol, respectively (Table 3). Total intermolecular, electrostatic and 'Hydrogen bond, Van der Waals and desolvation' energy values for this interaction were -9.42 kcal/mol, +0.12 kcal/mol and -9.54 kcal/mol, respectively. Thirteen amino acids (Ser70, Lys73, Tyr105, Pro107, Tyr129, Ser130, Asn132, Thr215, Thr216, Thr235, Gly236, Ser237, and Arg276) of CTX-M 15 enzyme interacted with para-biphenyl-2-methyl-3',5'-di-methylamide- $\alpha$ -D-mannoside.

Out of these 13 residues, Ser130, Ser237, and Arg276 were involved in hydrogen bonding while Ser70, Lys73, Tyr105, Pro107, Tyr129, Asn132, Thr215, Thr216, Thr235, and Gly236 were involved in hydrophobic interactions (Figure 2).

**Table 1:** Physicochemical properties of natural FimH inhibitors and control compound

Compound	Physicochemical parameter							
	Abs (%)**	Topological polar surface area (Å) <sup>2</sup>	Mol wt	cLogP***	Hydrogen bond donors	Hydrogen bond acceptors	No. of rotatable bonds	Lipinski's violation
Rule	-	-	<500	≤5	<5	<10	≤10	≤1
8-(Methoxycarbonyl)octyl-α-D-mannoside	65.64	125.68	350.40	0.545	4	8	12	1
Heptyl α-D-mannopyranoside	74.71	99.38	278.34	0.485	4	6	8	0
3'-Chloro-4'-(α-D-mannopyranosyloxy) biphenyl-4-carbonitrile	66.50	123.17	393.82	0.398	4	7	3	0
para-Biphenyl-2-methyl-3',5'-di-methyl amide-α-D-mannoside	54.63	157.58	460.48	0.205	6	10	6	1
para-Biphenyl- 2-methyl-3'-methyl amide mannoside	64.67	128.48	403.43	0.766	5	8	5	0
Thiazolylaminomannoside	31.78	223.82	465.51	-1.879	5	11	5	1
Aviabactam*	61.17	138.62	265.245	-2.688	2	9	3	0

\*Control CTX-M 15 inhibitor; \*\*Percentage of Absorption (% of Absorption) was calculated by: % of Absorption= 109 – [0.345 × Topological Polar Surface Area];

\*\*\*Logarithm of compound partition coefficient between *n*-octanol and water

**Table 2:** Toxicity potential of natural FimH inhibitors and control compound

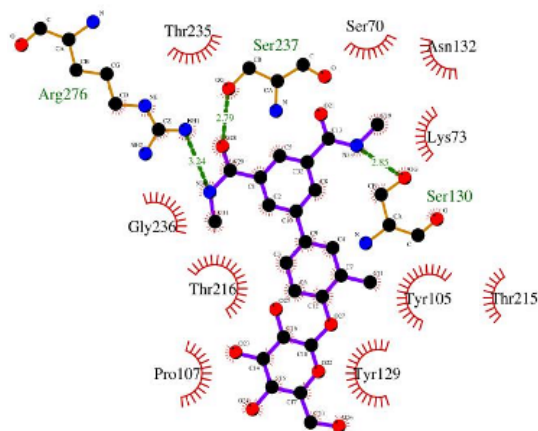
Compound	Toxicity risk			
	Mutagenic	Tumorigenic	Reproductive effect	Irritant
8-(Methoxycarbonyl)octyl-α-D-mannoside	None	None	None	None
Heptyl α-D-mannopyranoside	None	None	None	None
3'-Chloro-4'-(α-D-mannopyranosyloxy)biphenyl-4-carbonitrile	High	High	High	High
para-Biphenyl-2-methyl-3',5'-di-methylamide-α-D-mannoside	None	None	None	None
para-Biphenyl- 2-methyl-3'-methylamidemannoside	None	None	None	None
Thiazolylaminomannoside	None	None	None	None
Aviabactam*	High	None	High	None

\*Control CTX-M 15 inhibitor

**Table 3:** Molecular docking results of 'Cefotaximase-Munich 15 (CTX-M 15)' interaction with FimH inhibitor and control

Compound	Binding energy ( $\Delta G$ )	Inhibition constant ( $K_i$ )
8-(Methoxycarbonyloctyl- $\alpha$ -D-mannoside	-4.21kcal/mol	817.22mM
Heptyl $\alpha$ -D-mannopyranoside	-5.09kcal/mol	184.75mM
3'-Chloro-4'-( $\alpha$ -D-mannopyranosyloxy)biphenyl-4-carbonitrile	-7.46kcal/mol	3.38mM
para-Biphenyl-2-methyl-3',5'-di-methylamide- $\alpha$ -D-mannoside	-7.63kcal/mol	2.54mM
para-Biphenyl- 2-methyl-3'-methylamidemannoside	-7.47kcal/mol	3.35mM
Thiazolylaminomannoside	-7.63kcal/mol	2.57mM
Aviactam*	-6.23kcal/mol	26.99mM

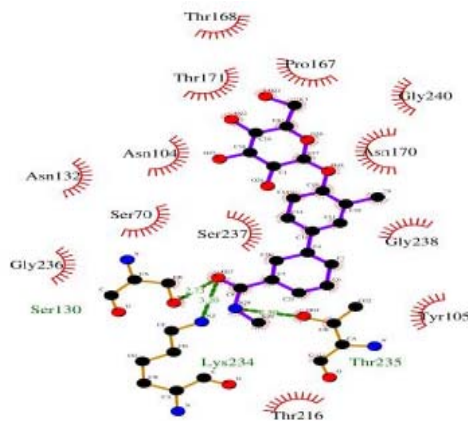
\*Control CTX-M 15 inhibitor

**Figure 2:** Ligplot analysis of 'para-biphenyl-2-methyl-3',5'-di-methylamide- $\alpha$ -D-mannoside' - 'CTX-M 15' interaction. Red arcs represents the amino acid involved in hydrophobic interactions, whereas, green dashed lines represents the hydrogen bonds along with bond lengths

The  $\Delta G$  and  $K_i$  values of para-biphenyl-2-methyl-3'-methylamidemannoside interaction with CTX-M 15 were -7.47 kcal/mol and 3.35 mM, respectively (Table 3). The intermolecular energy for this interaction was -8.96 kcal/mol. The total energy of Hydrogen bond, Van der Waals and Desolvation was -9.04 kcal/mol, while the energy for electrostatic bonding was +0.08 kcal/mol. CTX-M 15 amino acids Ser70, Asn104, Tyr105, Ser130, Asn132, Pro167, Thr168, Asn170, Thr171, Thr216, Lys234, Thr235, Gly236, Ser237, Gly238, and Gly240 interacted with para-biphenyl-2-methyl-3'-methylamidemannoside. Among these amino acid residues, Ser130, Lys234, and Thr235 were involved in hydrogen bonding, while the others were involved in hydrophobic interactions (Figure 3).

The  $\Delta G$  and  $K_i$  values for the interaction between thiazolylamino mannoside and CTX-M 15 were -7.63 kcal/mol and 2.57 mM, respectively (Table 3). The total energy of intermolecular was -9.42 kcal/mol, whereas, energy for electrostatic

bonding was -0.14 kcal/mol. The collective energy for hydrogen bond, Van der Waals interaction and desolvation was -9.28 kcal/mol. Seventeen amino acids (Ser70, Asn104, Tyr105, Ser130, Asn132, Pro167, Asn170, Thr171, Thr216, Ser220, Lys234, Thr235, Gly236, Ser237, Gly238, Gly240, and Arg276) of CTX-M 15 catalytic site interacted with thiazolylamino mannoside. Out of these amino acids, Ser70, Ser130, and Ser237 engaged in hydrogen bonding with thiazolylamino mannoside, while Asn104, Tyr105, Asn132, Pro167, Asn170, Thr216, Thr235, Gly236, Gly238, Gly240, and Arg276 were involved in hydrophobic interactions (Figure 4).

**Figure 3:** Ligplot analysis of 'para-biphenyl- 2-methyl-3'-methylamidemannoside' - 'CTX-M 15' interaction. Red arcs denote the amino acid involved in hydrophobic interactions, whereas, green dashed lines represents the hydrogen bonds along with bond lengths

For the aviactam (positive control)-CTX-M 15 interaction,  $\Delta G$  and  $K_i$  values were -6.23 kcal/mol and 26.99 mM, respectively (Table 3). Ser70, Lys73, Asn104, Tyr105, Ser130, Asn132, Thr216, Lys234, Thr235, Gly236, Ser237, and Arg276 were the twelve amino acid residues of the active site of CTX-M 15 that were involved in the aviactam-CTX-M 15 interaction. Most

importantly, six amino acid residues of CTX-M 15, i.e., Ser130, Asn132, Thr216, Thr235, Ser237, and Arg276 were involved in hydrogen bonding, while Ser70, Tyr105, and Gly236 were engaged in hydrophobic interactions (Figure 5).

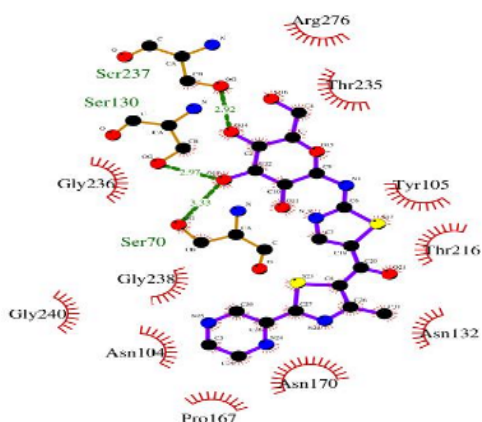


**Figure 4:** Ligplot analysis of 'thiazolylamino mannoside' - 'CTX-M 15' interaction. Red arcs denote the amino acid involved in hydrophobic interactions, whereas, green dashed lines represents the hydrogen bonds along with bond lengths

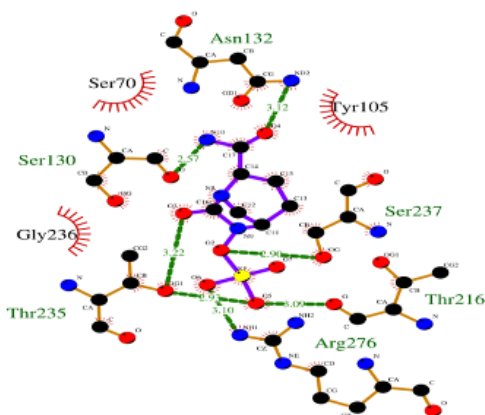


**Figure 5:** Ligplot analysis of 'Avibactam' - 'CTX-M 15' interaction. Red arcs denote the amino acid involved in hydrophobic interactions, whereas, green dashed lines represents the hydrogen bonds along with bond lengths

## DISCUSSION

Antibiotic resistance in uropathogenic bacteria due to ESBLs, especially CTX-M 15, has become a significant issue globally [4-6]. Thus, finding an alternative solution to this issue is a matter of great concern. Several studies have reported that uropathogenic bacteria belonging to Enterobacteriaceae family have been regarded as the primary causative agents for most UTI cases [3]. In addition, bacterial adherence to the host mucosal surface is a crucial step in any UTI

case, and the FimH produced by the Enterobacteriaceae family pathogens helps them attach to the mannosylated glycoproteins present on the epithelial cell surface of the urinary tract [8-10,21,22]. Therefore, FimH inhibitors might play an essential role in coping with the issues of antibiotic resistance by targeting cell adhesion without exhibiting bactericidal action. However, in the present study, the new potential of these FimH inhibitors was evaluated by assessing their CTX-M 15 inhibition potency. The present study outcomes might provide an add-on boost to over-the-counter antibiotics available for UTI treatment, by targeting both cell adhesion and ESBLs (CTX-M 15).

Among the FimH inhibitors, four inhibitors namely, 3'-chloro-4'-( $\alpha$ -D-mannopyranosyloxy) biphenyl-4-carbonitrile, para-biphenyl-2-methyl-3',5'-di-methylamide- $\alpha$ -D-mannoside, para-biphenyl-2-methyl-3'-methylamidemannoside, and thiazolylamino mannoside showed better interaction with CTX-M 15 than positive control avibactam when Gibbs free energy change ( $\Delta G$ ) were compared (Table 3). It is an entrenched fact that "ligand-target protein" interaction occurs only if the value of  $\Delta G$  is negative; in addition, high negative  $\Delta G$  also reflects enhanced affinity. Comparative analysis of interacting amino acids of all the molecular interactions showed that Ser70, Tyr105, Ser130, Asn132, Thr216, Thr235, Gly236, and Ser237 were the commonly interacting amino acids with both FimH inhibitors and avibactam. CTX-M 15 uses an acylation and deacylation process to hydrolyze  $\beta$ -lactam antibiotics. In fact, after the interaction between  $\beta$ -lactam antibiotics and CTX-M 15, the deacylation rate increases many-fold, leading to rapid CTX-M 15 regeneration. In addition, CTX-M 15 inhibitor forms strong acyl-enzyme complex bonding, thus reducing the deacylation or regeneration efficacy of CTX-M 15. Hence, CTX-M 15 inhibitor efficiency is measured by low deacylation and high acylation rates of CTX-M 15 [23].

Structure-activity relationship studies have shown the importance of Ser70 and Ser130 during the acylation process of CTX-M 15 by their inhibitors [7,24]. In the present work, two amino acid residues, Ser70 and Ser130, found in the CTX-M 15 active site commonly interacted with the FimH inhibitors. Thus, the FimH inhibitors tested in this study could be further explored as CTX-M 15 inhibitors as well. Further experimental validations are needed to ascertain the CTX-M 15 inhibition potential of FimH inhibitors and to convert them as dual inhibitors of FimH and CTX-M 15 enzyme. However, *in silico* findings have been reported to often

correlate well with wet-lab outcomes. The preliminary findings of the present study suggest a plausible alternate strategy for combating the current resistance issues caused by CTX-M 15-producing uropathogenic bacterial strains.

## CONCLUSION

FimH inhibitors are currently under development for their use against adherence of uropathogenic bacterial strains to host cells. In the present study, FimH inhibitors were docked to CTX-M 15 enzyme to predict their dual targeting potential. Interestingly, they have shown better interaction with the catalytic site of CTX-M 15 than positive control. This would provide an add-on advantage to the ongoing research on FimH inhibitors, in order to develop them as alternative antibacterial therapy candidates. In addition, the findings of this study would help researchers to design more versatile and potent CTX-M 15 inhibitors to cope with the antibiotic resistance issues of uropathogenic bacteria more effectively.

## DECLARATIONS

### Conflict of Interest

No conflict of interest associated with this work.

### Contribution of Authors

The authors declare that this work was done by the authors named in this article and all liabilities pertaining to claims relating to the content of this article will be borne by them.

### Open Access

This is an Open Access article that uses a funding model which does not charge readers or their institutions for access and distributed under the terms of the Creative Commons Attribution License (<http://creativecommons.org/licenses/by/4.0>) and the Budapest Open Access Initiative (<http://www.budapestopenaccessinitiative.org/read>), which permit unrestricted use, distribution, and reproduction in any medium, provided the original work is properly credited.

## REFERENCES

- Gonzalez CM, Schaeffer AJ. Treatment of urinary tract infection: what's old, what's new, and what works. *World J Urol* 1999;17(6): 372-82.
- Huh JS. The prevalence of urinary tract infections in institutionalized vs. noninstitutionalized elderly persons. *Urogenital Tract Infection* 2016; 11(2): 56-61.
- Ronald A, Nicolle L, Stamm E, Krieger J, Warren J, Schaeffer A, Naber K, Hooton T, Johnson J, Chambers S. Urinary tract infection in adults: research priorities and strategies. *Internat J antimicrob agent* 2001; 17(4): 343-348.
- Paterson DL, Bonomo RA. Extended-spectrum beta-lactamases: a clinical update. *Clin Microbiol Rev* 2005; 18(4): 657-86.
- Mathers AJ, Peirano G, Pitout JD. The role of epidemic resistance plasmids and international high-risk clones in the spread of multidrug-resistant Enterobacteriaceae. *Clin Microbiol Rev* 2015; 28(3): 565-91.
- Jasper RT, Coyle JR, Katz DE, Marchaim D. The complex epidemiology of extended-spectrum beta-lactamase-producing Enterobacteriaceae. *Future Microbiol* 2015; 10(5): 819-39.
- Lahiri SD, Mangani S, Durand-Reville T, Benvenuti M, De Luca F, Sanyal G, Docquier JD. Structural insight into potent broad-spectrum inhibition with reversible recyclization mechanism: avibactam in complex with CTX-M-15 and *Pseudomonas aeruginosa* AmpC beta-lactamases. *Antimicrob Agents Chemother* 2013; 57(6): 2496-505.
- Edén CS, Hagberg L, Hanson LÅ, Hull S, Hull R, Jodal U, Leffler H, Lomberg H, Straube E. Bacterial adherence—a pathogenetic mechanism in urinary tract infections caused by *Escherichia coli*. *Host Parasite Relationships in Gram-Negative Infections* 1983; 33: 175-88.
- Krammer EM, De Ruyck J, Roos G, Bouckaert J, Lensink MF. Targeting dynamical binding processes in the design of non-antibiotic anti-adhesives by molecular simulation—the example of FimH. *Molecules* 2018; 23(7): 1641.
- Stahlhut SG, Tchesnokova V, Struve C, Weissman SJ, Chattopadhyay S, Yakovenko O, Aprikian P, Sokurenko EV, Krogfelt KA. Comparative structure-function analysis of mannose-specific FimH adhesins from *Klebsiella pneumoniae* and *Escherichia coli*. *J Bacteriol* 2009; 191(21): 6592-601.
- Connell I, Agace W, Klemm P, Schembri M, Märdil S, Svanborg C. Type 1 fimbrial expression enhances *Escherichia coli* virulence for the urinary tract. *Proc Natl Acad Sci U S A* 1996; 93(18): 9827-32.
- Mulvey MA, Lopez-Boado YS, Wilson CL, Roth R, Parks WC, Heuser J, Hultgren SJ. Induction and evasion of host defenses by type 1-piliated uropathogenic *Escherichia coli*. *Science* 1998; 282(5393): 1494-7.
- Rosen DA, Pinkner JS, Walker JN, Elam JS, Jones JM, Hultgren SJ. Molecular variations in *Klebsiella pneumoniae* and *Escherichia coli* FimH affect function and pathogenesis in the urinary tract. *Infect Immun* 2008; 76(7): 3346-56.
- Struve C, Bojer M, Krogfelt KA. Characterization of *Klebsiella pneumoniae* type 1 fimbriae by detection of phase variation during colonization and infection and impact on virulence. *Infect Immun* 2008; 76(9): 4055-65.
- Bouckaert J, Berglund J, Schembri M, De Genst E, Cools L, Wuhler M, Hung CS, Pinkner J, Slättegård R, *Trop J Pharm Res*, November 2021; 20(11): 2369

- Zavialov A, Choudhury D. Receptor binding studies disclose a novel class of high-affinity inhibitors of the *Escherichia coli* FimH adhesin. *Mol Microbiol* 2005; 55(2): 441-55.
16. Bouckaert MLJ. Molecular mechanisms of drug action: X-ray crystallography at the basis of structure-based and ligand-based drug design. *Biophys Tech Drug Dis* 2017; 61: 67.
  17. Mydock-McGrane LK, Hannan TJ, Janetka JW. Rational design strategies for FimH antagonists: new drugs on the horizon for urinary tract infection and Crohn's disease. *Expert Opin Drug Discov* 2017; 12(7): 711-31.
  18. Lipinski CA, Lombardo F, Dominy BW, Feeney PJ. Experimental and computational approaches to estimate solubility and permeability in drug discovery and development settings. *Advanced Dru Deliv Rev* 1997; 23(1-3): 3-25.
  19. Zhao YH, Abraham MH, Le J, Hersey A, Luscombe CN, Beck G, Sherborne B, Cooper I. Rate-limited steps of human oral absorption and QSAR studies. *Pharmaceut Res* 2002; 19(10): 1446-57.
  20. Rizvi SM, Shakil S, Haneef M. A simple click by click protocol to perform docking: AutoDock 4.2 made easy for non-bioinformaticians. *EXCLI J* 2013; 12: 831-57.
  21. Zhou K, Lokate M, Deurenberg RH, Arends J, Foe LT, Grundmann H, Rossen JW, Friedrich AW. Characterization of a CTX-M-15 producing *Klebsiella pneumoniae* outbreak strain assigned to a novel sequence type (1427). *Front Microbiol* 2015; 6: 1250.
  22. Zhou G, Mo WJ, Sebbel P, Min G, Neubert TA, Glockshuber R, Wu XR, Sun TT, Kong XP. Uroplakin Ia is the urothelial receptor for uropathogenic *Escherichia coli*: evidence from *in vitro* FimH binding. *J Cell Sci* 2001; 114(22): 4095-103.
  23. Faheem M, Rehman MT, Danishuddin M, Khan AU. Biochemical characterization of CTX-M-15 from *Enterobacter cloacae* and designing a novel non- $\beta$ -lactam- $\beta$ -lactamase inhibitor. *PLoS One* 2013; 8(2): e56926.
  24. King DT, King AM, Lal SM, Wright GD, Strynadka NC. Molecular mechanism of avibactam-mediated  $\beta$ -lactamase inhibition. *ACS Infect Dis* 2015; 1(4): 175-184.